IEEE Access
Multidisciplinary ⋮ Rapid Review ⋮ Open Access Journal

Received June 5, 2020, accepted June 19, 2020, date of publication July 2, 2020, date of current version July 14, 2020.

Digital Object Identifier 10.1109/ACCESS.2020.3006522

DeCoNet: Density Clustering-Based Base Station Control for Energy-Efficient Cellular IoT Networks

WONSEOK LEE[1], BANG CHUL JUNG[2], (Senior Member, IEEE), AND HOWON LEE[3], (Member, IEEE)

[1]Innovative Technology Lab (ITL) Inc., Seoul 06744, South Korea
[2]Department of Electronics Engineering, Chungnam National University, Daejeon 34134, South Korea
[3]School of Electronic and Electrical Engineering and IITC, Hankyong National University, Anseong 17579, South Korea

Corresponding author: Howon Lee (hwlee@hknu.ac.kr)

This work was supported in part by the National Research Foundation of Korea (NRF) grant funded by the Korean Government (MSIT) under Grant 2019R1F1A1063606 and in part by the NRF through the Basic Science Research Program funded by the Ministry of Science and ICT under Grant NRF2019R1A2B5B01070697.

ABSTRACT Recently, there has been a rapid increase in the number of (small-cell) base stations (BSs) to support the massive amount of mobile data traffic and rapidly increasing number of mobile devices in beyond 5G (B5G) wireless communication systems or Internet of Things (IoT) networks. However, many of these BSs tend to waste a considerable amount of energy to support such data traffic and mobile devices. Therefore, the development of an efficient BS status control algorithm is important for realizing energy-efficient IoT networks. To reduce network energy consumption, we herein propose a density clustering-based BS control algorithm for energy-efficient IoT networks (DeCoNet). DBSCAN (Density-Based Spatial Clustering of Applications with Noise) and OPTICS (Ordering Points To Identify the Clustering Structure) are utilized for partitioning high and low user-density regions. To find the effective number of BSs and their appropriate locations considering user-density differences, we utilize parameters obtained after applying density clustering algorithms to derive the thinning radius that is used to adjust the status of BSs in overall cellular IoT networks. Specifically, the average reachability-distance of each cluster in OPTICS and the distance between the outermost border users of each cluster in DBSCAN are used to obtain the radius of each cluster region. Through extensive computer simulations, we show that the proposed algorithms outperform the conventional algorithms in terms of average area throughput, energy efficiency, energy per information bit, and power consumption per unit area.

INDEX TERMS Density clustering, ultra-dense network, energy efficiency, thinning algorithm, cellular IoT networks, BS control.

I. INTRODUCTION

Future wireless networks such as the beyond fifth generation 5G (B5G) system or Internet of Things (IoT) system aim at supporting the rapidly increasing number of mobile devices and data traffic while reducing the network energy consumption compared to the fourth generation (4G) networks [1]. The B5G system will essentially help to establish the IoT as an indispensable part of our lives by setting up the foundation for unleashing its full potential [2], [3]. To achieve this goal, energy-efficient ultra-dense networks (UDNs) have been widely regarded as one of the most promising solutions for the future wireless networks [4]–[6]. In other words, base stations (BSs) may be deployed more densely to support the massive amount of data traffic generated by the various B5G convergence services such as smart factories, smart cities, smart homes, drone deliveries, and autonomous driving. Accordingly, the average distance between users and BSs is exponentially reducing, and therefore the link quality and network capacity could be enhanced significantly. However, this may result in severe interference among neighboring BSs, ushering in a vast amount of energy waste in the entire network [7]–[9]. Hence, reducing the network energy consumption is one of the most challenging issues for realizing UDNs in practice, particularly given that 80% of the energy in mobile networks is consumed in BSs [10], [11].

To minimize the network energy consumption in UDNs, a scheme to adjust the mode of BSs as (*awake* or *sleep*) was proposed in [12]. Furthermore, in [13], potential gains and limitations of the UDNs were studied,

The associate editor coordinating the review of this manuscript and approving it for publication was Yue Zhang.

which addressed the impact of idle-mode operation of BSs, transmission power of BSs, user density, and user distribution on the energy efficiency of UDNs. In [14], a centralized on/off optimization technique was proposed by using system-level simulations for heterogeneous networks. In [15], a Markov decision process (MDP)-based optimal wake-up mechanism for femto-cell BSs was proposed to minimize the energy consumption of heterogeneous networks, and in [16], energy-efficient user association and power allocation methods were proposed for mmWave-based UDNs with energy-harvesting BSs. Furthermore, Z. Jian *et al.* proposed a joint optimization framework for an energy-efficient switching on/off strategy and user association policy in dense cellular networks with partial conventional BSs in [17], and traffic load distribution-based on/off scheduling algorithms were proposed for energy-efficient delay-tolerant 5G networks in [18].

On the other hand, clustering techniques can be used for improving the network energy efficiency in UDNs by efficiently partitioning the BSs and users according to the density, position, etc. In [19], Liang *et al.* proposed a cluster-based energy-efficient resource allocation scheme for UDNs to reduce interference and boost energy efficiency. They utilized the k-means clustering algorithm to dynamically adjust the number of BS-clusters based on the density of the BSs. Moreover, [20] used a modularity-based user-centric clustering to decompose the UDNs into several sub-networks by exploiting the inherent group structure of users. However, they did not consider the user density for adjusting the modes of BSs in the UDNs. In this paper, to further improve network energy efficiency, we propose a novel density clustering-based BS control algorithm for energy-efficient (ultra-dense) cellular IoT networks (DeCoNet). DBSCAN (Density-Based Spatial Clustering of Applications with Noise) and OPTICS (Ordering Points To Identify the Clustering Structure) are utilized for partitioning the users in the proposed DeCoNet algorithms. The main contribution of this paper is to partition high and low user-density regions to efficiently control the mode of BSs by using DBSCAN and OPTICS algorithms. After extracting the high user-density regions, a mobile network operator is able to determine the number and location of BSs to be awakened. The radii of the high user-density regions can be obtained by using the parameters found through the results of DBSCAN and OPTICS. We can find the thinning radius that is used to adjust the status of the BSs based on the distance between the outermost nodes in DBSCAN-based DeCoNet (D-DeCoNet) and the reachability-distance in OPTICS-based DeCoNet (O-DeCoNet). This paper also uses a thinning operation to apply area-based BS control algorithms for energy-efficient cellular IoT networks.

The rest of this paper is organized as follows. The Poisson point process (PPP) and thinning operation are described in Section II. Two density-based clustering algorithms are introduced in Section II: DBSCAN and OPTICS. In Section III, the proposed DeCoNet algorithms are explained. Section IV shows the simulation results in terms of the average area throughput, energy efficiency, energy per information bit, and power consumption per unit area. Finally, the conclusions are drawn in Section V.

II. PRELIMINARIES

A. POISSON POINT PROCESS (PPP) AND THINNING OPERATION

In PPP, the cumulative density function (CDF, $F_r(R)$) of the distance between the nearest serving BS and the user (r) can be represented as [7], [21]

$$\begin{aligned} F_r(R) &= \mathbb{P}[\textit{Number of BSs closer than } R] \\ &= \mathbb{P}[r \le R] \\ &= 1 - e^{-\lambda_B \pi R^2}. \end{aligned} \tag{1}$$

Here, λ_B represents the BS intensity of the two-dimensional PPP defined in the specific space with a radius R. From Eqn. (1), we can calculate the probability density function (PDF) of r in the homogeneous PPP ($f_r(r)$) as

$$f_r(r) = 2\pi\lambda_B r \cdot e^{-\lambda_B \pi r^2}. \tag{2}$$

In this paper, we denote the PDFs of r in the homogeneous PPP and Matérn hard core point process (HCPP) as $f_{r.p}(r)$ and $f_{r.t}(r)$, respectively. The thinning operation in the HCPP creates a group of new points by removing the points within the thinning radius (r_t) on the basis of reference points among all the original points generated by the homogeneous PPP. In this study, the thinning operation removes the points according to the following steps [7]:

- **Step 1:** Assign a random marked value (M) between 0 and 1 for all the points sampled by the PPP.
- **Step 2:** Find the points within r_t on the basis of the reference point, and remove the points with a smaller marked value than the reference point.
- **Step 3:** Repeat Step 1 and Step 2 for all the points in the entire network.

Accordingly, the intensity of the BS in the network is altered, and the PDF of the distance r between the BS and the user is also changed. In this case, the PDF of r after applying the thinning operation can be approximated as [7], [23], [24]

$$f_{r.t}(r) \approx 2\pi r\lambda_B \frac{1 - e^{-\lambda_B \pi r_t^2}}{\lambda_B \pi r_t^2} e^{-\lambda^s \mathsf{A}(r, r_t)}, \tag{3}$$

where the intensity of the remaining BSs after the thinning operation can be expressed as $\lambda_{B.t} = (1 - e^{-\lambda_B \pi r_t^2})/\pi r_t^2$ [7], [25]–[27]. In Eqn. (3), λ^s is a unique value that matches the sum of the PDF to 1. In addition, $\mathsf{A}(r, r_t)$ in Eqn. (3) can be described as follows [7], [23]:

$$\mathsf{A}(r, r_t) = \begin{cases} 0 & 2r \le r_t \\ \pi r^2 + r_t\sqrt{r^2 - \dfrac{r_t^2}{4}} & \\ -(2 \cdot \arcsin\dfrac{r_t}{2r} + \arccos\dfrac{r_t}{2r}) \times r^2, & 2r > r_t \end{cases} \tag{4}$$

$N(r_i)$ is the average number of users within the ith integration region. The entire space $\mathbf{S}$ in the PPP can be quantized into bins with bounds $(r_i - \Delta r/2, r_i + \Delta r/2)$, where $r_i = r_0 + i \cdot \Delta r$ for $i \in \mathbb{Z}^+$ [8]. Here, we assume that r_0 is a clearance region, where no user is located. Therefore, $N(r_i)$ of the ith integration region, whose area is $2\pi r_i \Delta_r$, can be expressed as [7]–[9]

$$N(r_i) = \sum_k k \cdot \frac{(\lambda_u 2\pi r_i \Delta r)^k}{k!} e^{-\lambda_u 2\pi r_i \Delta r}, \quad k \in \mathbb{Z}^+. \tag{5}$$

Here, λ_u denotes the user intensity in PPP. From Eqns. (2) and (5), we can calculate the total number of users within the BS coverage area. Therefore, the number of users in the BS coverage area ($N_{u.tot}$) is approximately calculated as

$$N_{u.tot} = \sum_i p_r(r_i) \cdot N(r_i), \tag{6}$$

where the probability mass function $p_r(r_i)$ can be calculated as $p_r(r_i) = \int_{r_i-\Delta r}^{r_i+\Delta r} f_r(r)dr$. In addition, in accordance with [7] and [22], the average number of users within the coverage area of each BS ($N_{u.tot}$) can be expressed as $\frac{\lambda_u}{\lambda_B}$.

B. DENSITY-BASED CLUSTERING ALGORITHM

To achieve efficient control of a large number of BSs, network operators might partition the entire network area in accordance with active user density. Accordingly, user density-based clustering algorithms could be utilized for network partitioning. We herein introduce two of the representative clustering algorithms utilizing user density, namely, DBSCAN and OPTICS. In general, density-based clustering is used to extract regions having the desired user density or a higher distribution of objects (data or points). Several key terminologies used in the DBSCAN and OPTICS algorithms are summarized as follows [28], [29].

- **Directly density-reachable:** When an object o has at least *MinPts* of other objects $(p_1, p_2, p_3 \ldots)$ within a radius (ε), we assume that the objects p_1, p_2, and p_3 are directly density-reachable from the object o. Here, *MinPts* denotes the minimum number of objects to form a dense region.
- **Density-reachable:** Assume that the objects p_1, p_2, and p_3 are directly density-reachable from o_1, and q_1, q_2, and q_3 are directly density-reachable from o_2. If the core objects o_1 and o_2 are directly density-reachable, we assume that q_1, q_2, and q_3 are density-reachable from o_1.
- **Density-connected:** If the objects p and q are density-reachable from object o, we assume that the objects p and q are density-connected.

1) DBSCAN

DBSCAN creates several clusters of indefinite shape according to the density of the neighboring objects. In DBSCAN, there exist three kinds of objects, namely, a core object, a border object, and an outlier object [28]. The descriptions for these nodes are as follows.

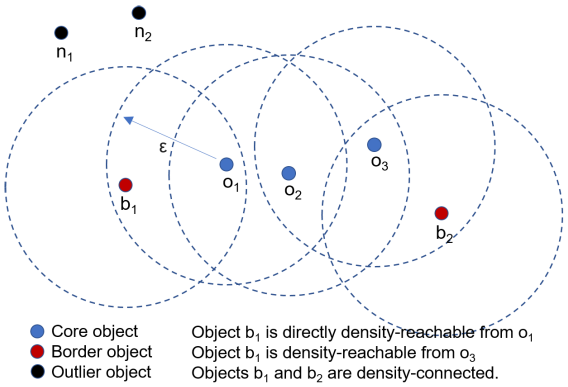

FIGURE 1. DBSCAN operation procedure with radius ε when *MinPts* = 3.

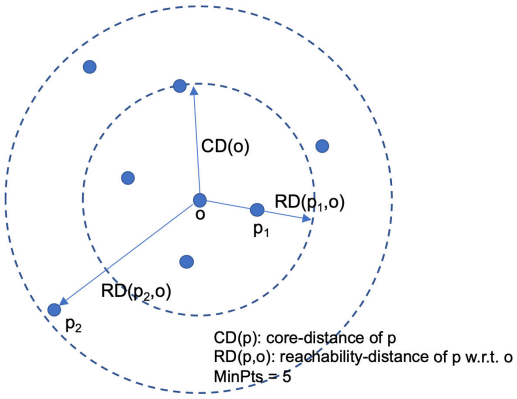

FIGURE 2. Core-distance and reachability-distance in OPTICS.

- **Core object:** When an object o has at least *MinPts* of other objects $(p_1, p_2, p_3 \ldots)$ within ε, the point o is a *core object*. In Fig. 1, the objects o_1, o_2, and o_3 are the core objects.
- **Border object:** As shown in Fig. 1, the objects b_1 and b_2 are not core objects but are within ε of any core object. These objects are assumed to be border objects.
- **Outlier object:** The objects n_1 and n_2 in Fig. 1 do not satisfy the requirements of core object or border object. These objects are assumed to be outlier objects.

Fig. 1 shows the operation procedure of DBSCAN when *MinPts* = 3. Objects o_1, o_2, and o_3 are core objects because they have more than *MinPts* objects within a radius (ε). Basically, the core objects form a cluster. Thus, density-reachable objects from the core object are merged into a cluster. That is, the objects o_1, o_2, and o_3 form a cluster. Furthermore, the border objects belong to the cluster composed of directly density-reachable objects from the core object. Hence, b_1 belongs to the cluster formed by o_1, and b_2 belongs to the cluster formed by o_3, as shown in Fig. 1. The outlier objects n_1 and n_2 are excluded from forming clusters because they are not density-reachable or density-connected.

2) OPTICS

OPTICS defines the *MinPts*-distance of an object p, core-distance (CD) of an object p, and reachability-distance (RD) of an object p with respect to an object o [29].

Here, *MinPts*-distance represents the distance from p to its *MinPts*' neighbors, and usually this *MinPts*-distance is the same as the CD when the ε-neighborhood of p is greater than *MinPts*. The CD of p can be defined as

$$CD(p) = \begin{cases} \text{Undefined}, & \varepsilon\text{-neighborhood}(p) \\ & < MinPts \\ Minpts - \text{distance}(p), & \text{otherwise.} \end{cases} \quad (7)$$

The reachability-distance of an object p with respect to another object o is the smallest distance such that p is directly density-reachable from the core object o. That is, according to the definition, the reachability-distance cannot be smaller than the core-distance. The reachability-distance can be defined as

$$RD(p, o) = \begin{cases} \text{Undefined}, & \varepsilon\text{-neighborhood}(p) \\ & < MinPts \\ \max(CD(o), \text{dist}(o, p)) & \text{otherwise.} \end{cases} \quad (8)$$

Fig. 2 shows an example of the core-distance ($CD(o)$) and the reachability-distance ($RD(p_1, o)$, $RD(p_2, o)$) when $MinPts = 5$. Accordingly, OPTICS can efficiently extract the boundaries of each cluster in the entire network area by using the reachability-distance plot [29].

III. DeCoNet: PROPOSED DENSITY CLUSTERING-BASED BS CONTROL ALGORITHM

In the proposed DeCoNet algorithm, the entire network is divided into several subnetworks, and the status of each BS is determined according to the condition of each subnetwork. To partition the entire network, the users can be classified using the density-based clustering algorithms such as DBSCAN and OPTICS, described in Sec.II-B1 and Sec.II-B2, respectively. As a result, each cluster formed by the clustering algorithms is mapped to each subnetwork. Each subnetwork obtains the thinning radius (r_t) based on the clustering results (the number of users and a cluster radius (r_c)) for determining the awake/sleep mode of the BS. The proposed DeCoNet algorithm for improving energy efficiency in ultra-dense IoT networks performs the following procedures.

As shown in Step 1 in Algorithm 1, BSs and users are generated within the entire network area with λ_B and λ_u^L, where λ_B and λ_u^L denote the intensities of the BSs and users in the low-density area, respectively. To model crowded network environments such as a stadium or a shopping mall, high user-density regions are randomly distributed within the entire network area, and the users in the high-density region are generated with λ_u^H, as shown in Step 2. The density-based user clustering algorithm (DBSCAN or OPTICS) divides the entire network into multiple subnetworks. Network area partitioning is performed to determine the number of BSs that need to be awake in each subnetwork. In other words, OPTICS and DBSCAN extract the dense areas in the entire network area to control the BSs according to the number of active users for improving the network energy efficiency while minimizing the cell throughput degradation.

In Step 3, the users are partitioned using OPTICS in O-DeCoNet and DBSCAN in D-DeCoNet. That is, the subnetworks are extracted using density-based clustering algorithms. In Algorithm 1, Option 1 represents the steps to extract subnetworks in O-DeCoNet. In Step 3.1, each user calculates the *MinPts*-distance to find the core-distance ($CD_{i\in\mathbb{S}_u}$) of itself. Then, O-DeCoNet randomly selects the first user i in $\mathbb{S}_u$ and defines new sets $\mathbb{S}^{\text{SEED}} = \mathbb{S}_u$ and $\mathbb{S}^{\text{ORDER}} = \emptyset$. After comparing $\text{Dist}(i,j)_{j\in_{j\neq i}\mathbb{S}_u}$ with CD_i, the larger value will be set to a temporary-value TV_k for all k in Step 3.3. Here, $\text{Dist}(i,j)_{j\in_{j\neq i}\mathbb{S}_u}$ denotes the distance between the i-th user and other users in $\mathbb{S}_u$. In Step 3.4, O-DeCoNet compares the current reachability-distance (RD_k) with the temporary-value (TV_k) and sets the smaller value as the final reachability-distance (RD_k) for all k. Then, user i is removed from $\mathbb{S}^{\text{SEED}}$ and added to $\mathbb{S}^{\text{ORDER}}$ in Step 3.5. In Step 3.6, the user i with the smallest *RD* is determined as the next i, and the steps from 3.3 to 3.6 are repeated until $\mathbb{S}^{\text{SEED}}$ becomes empty. The point $j+1$ satisfying $RD_j^{\mathbb{S}^{\text{ORDER}}} \times (1-\xi) \geq RD_{j+1}^{\mathbb{S}^{\text{ORDER}}}$ becomes the start point of the cluster i, $\mathbb{S}_u^{\text{i,start}}$, and the point k satisfying $RD_k^{\mathbb{S}^{\text{ORDER}}} \leq RD_{k+1}^{\mathbb{S}^{\text{ORDER}}} \times (1-\xi)$ becomes the end point of the cluster i, $\mathbb{S}_u^{\text{i,end}}$. In Step 3.8, if k - $j \geq MinPts$, all successive users between $\mathbb{S}_u^{\text{i,start}}$ and $\mathbb{S}_u^{\text{i,end}}$ form a new cluster. Particularly in OPTICS, the size of the extracted high user-density regions can be controlled by the parameter ξ. For example, if we strictly set the value of ξ, the area throughput of O-DeCoNet could be smaller but the energy efficiency of O-DeCoNet could be higher, and vice versa.

Option 2 represents how to extract subnetworks in D-DeCoNet. In Step 3.1, when user i has at least *MinPts* of other users within ε, the user i is set as 'core user' for all i. If a certain core user i is located within ε of another core user j, then the users i and j are set as 'density-connected' users in Step 3.2. The D-DeCoNet extracts these density-connected users into a cluster. In Step 3.4, the users who do not satisfy the condition of a core user but are within ε of another core user are set as border users. The border users ($\mathbb{S}_u^{i,b}$) are also included in the same cluster (i) with these core users in Step 3.5. After applying density-based clustering algorithms, unique output parameters can be obtained. In OPTICS, RD and CD for each user are obtained. Furthermore, in DBSCAN, the type of user (core, border, outlier) is determined. Fig. 5 shows an example of an RD plot in O-DeCoNet.

After clustering the users with RD_i in OPTICS and the distance between the outermost border users in DBSCAN, the proposed DeCoNet algorithm can find the radius of each cluster (r_c). In O-DeCoNet, we can find that *RD* values of each cluster are similar. This finding means that the average *RD* value for each cluster could be the radius of the cluster region. Consequently, we can obtain r_c by averaging all the *RD* values in each cluster. In addition, r_c can be calculated

Algorithm 1 Operation Procedures of O-DeCoNet and D-DeCoNet

[Network configuration for BSs and users]

Step 1. The sets of BSs ($\mathbb{S}_B$) and users ($\mathbb{S}_u$) are generated by the Poisson point process with λ_B and λ_u^L. Here, λ_u^L is the intensity of the Poisson point process for the lower user-density area.

Step 2. The higher user-density areas are generated by the Poisson cluster process with λ_u^H, and these areas are randomly located in the entire network area. The size of the entire network is $1\,\mathrm{km}^2$.

Step 3. Apply a density-based clustering algorithm for constructing the subnetworks with O-DeCoNet or D-DeCoNet.

[Option 1: O-DeCoNet - OPTICS based BS control algorithm]

Step 3.1. Every user calculates the *MinPts*-distance for finding $CD_{i\in\mathbb{S}_u}$.

Step 3.2. Randomly select the first user i in $\mathbb{S}_u$, and define $\mathbb{S}^{\mathrm{SEED}} = \mathbb{S}_u$ and $\mathbb{S}^{\mathrm{ORDER}} = \emptyset$.

Step 3.3. Compare $\mathrm{Dist}(i,j)_{j\in_{j\neq i}\mathbb{S}_u}$ with CD_i, where $\mathrm{Dist}(i,j)_{j\in_{j\neq i}\mathbb{S}_u}$ is the distance between i and other users in $\mathbb{S}_u$. The larger value will be set to TV_k, where k is all users.

Step 3.4. Compare the current RD_k with TV_k and set the smaller value as the final RD_k for all k.

Step 3.5. Remove i from $\mathbb{S}^{\mathrm{SEED}}$ and add it to $\mathbb{S}^{\mathrm{ORDER}}$.

Step 3.6. The user i with the smallest RD is determined as the next i, and the steps from 3.3 to 3.6 are repeated until $\mathbb{S}^{\mathrm{SEED}}$ becomes empty.

Step 3.7. Find $\mathbb{S}_u^{\mathrm{i,start}}$ satisfying $RD_j^{\mathbb{S}^{\mathrm{ORDER}}} \times (1-\xi) \geq RD_{j+1}^{\mathbb{S}^{\mathrm{ORDER}}}$, and $\mathbb{S}_u^{\mathrm{i,end}}$ satisfying $RD_k^{\mathbb{S}^{\mathrm{ORDER}}} \leq RD_{k+1}^{\mathbb{S}^{\mathrm{ORDER}}} \times (1-\xi)$.

Step 3.8. If k - $j \geq MinPts$, all successive users between $\mathbb{S}_u^{\mathrm{i,start}}$ and $\mathbb{S}_u^{\mathrm{i,end}}$ form a new cluster..

[Option 2: D-DeCoNet - DBSCAN based BS control algorithm]

Step 3.1. When user i has at least *MinPts* of other users within ε, the user i is set as 'core user' for all i.

Step 3.2. If a certain core user i is within ε of another core user j, these users are set as 'density-connected' users.

Step 3.3. The density-connected users are extracted into a cluster.

Step 3.4. The users not satisfying the condition of core user but are within ε of another core user are set as border users.

Step 3.5. The border users ($\mathbb{S}_u^{i,b}$) are also included in the same cluster (i) with these core users.

[Thinning radius (r_t) calculation and mode control of BSs]

Step 4. To calculate r_c^i, O-DeCoNet uses the average value of $RD_{\mathbb{S}_u^{\mathrm{i,start}}\_\mathrm{to}\_\mathbb{S}_u^{\mathrm{i,end}}}$ of the ith cluster, and D-DeCoNet uses the distance between ($\mathbb{S}_u^{i,b}$) in the ith cluster.

Step 5. r_t^i can be expressed as $r_t^i = \sqrt{\frac{(r_c^i)^2}{N_{\mathrm{B}}^{i,\mathrm{awake}}}}$, where $N_{\mathrm{B}}^{i,\mathrm{awake}} = \frac{\mathrm{Card}(\mathbb{S}_u^i)}{\mu_B}$. Here, Card is the size of the set.

Step 6. Based on the calculated r_t^i, the modes of neighboring BSs within a distance of r_t^i from the specific BS are changed from awake to sleep in cluster i. Here, the specific BS is randomly chosen among the awake BSs.

Step 7. Steps 4 to 6 are repeated for all clusters.

using the distance between the outermost border users in D-DeCoNet. In O-DeCoNet and D-DeCoNet, the radius of a cluster i (r_c^i) can be obtained as

$$r_c^i = \begin{cases} \sum_{k=\mathbb{S}_u^{\mathrm{i,start}}}^{\mathbb{S}_u^{\mathrm{i,end}}} \frac{RD_k}{\mathrm{Card}(\mathbb{S}_u^i)} & \text{in O-DeCoNet,} \\ \arg_{j,k\in\mathbb{S}_u^{i,b}} \max \frac{\mathrm{Dist}(j,k)}{2} & \text{in D-DeCoNet.} \end{cases} \quad (9)$$

In Eqn. (9), $\mathrm{Card}(\mathbb{S}_u^i)$ indicates the number of users in cluster i. The terms $\mathbb{S}_u^{\mathrm{i,start}}$ and $\mathbb{S}_u^{\mathrm{i,end}}$ indicate the order of the start- and end-user of cluster i, respectively, where order is a unique number of a user belonging to each cluster in the RD plot.

Therefore, the thinning radius of the cluster i (r_t^i) for controlling the modes of BSs can be calculated as

$$r_t^i = \sqrt{\frac{(r_c^i)^2}{N_{\mathrm{B}}^{i,\mathrm{awake}}}} \quad \text{where} \quad N_{\mathrm{B}}^{i,\mathrm{awake}} = \frac{\mathrm{Card}(\mathbb{S}_u^i)}{\mu_B}. \quad (10)$$

In Eqn. (10), the number of BSs that need to be awakened ($N_{\mathrm{B}}^{i,\mathrm{awake}}$) can be derived by dividing $\mathrm{Card}(\mathbb{S}_u^i)$ by μ_B. Here, $\mathrm{Card}(\mathbb{S}_u^i)$ is the number of users included in the cluster i, and μ_B is the capacity of the BS. The capacity of the BS is the number of users that can be supported through the BS. In Step 6 in Algorithm 1, with the r_t^i by Eqn. (10), the modes of neighboring BSs within a distance of r_t^i from the specific BS are changed from awake to sleep in the cluster i. A different value of r_t could be applied for each subnetwork in accordance with the user density. A block diagram of the proposed DeCoNet algorithm is shown in Fig. 3.

In Fig. 4, there are three clustered areas and one non-clustered area. Therefore, we finally have four subnetworks that have different user densities. The thinning process of the proposed DeCoNet algorithm is shown in Fig. 4. Here, there are three kinds of users, namely, a core user, a border user, and an outlier user. The core and border users are those users included in each cluster, while the outlier users are the nonclustered users. One of the border users can be considered as the outermost user to determine the size of each cluster

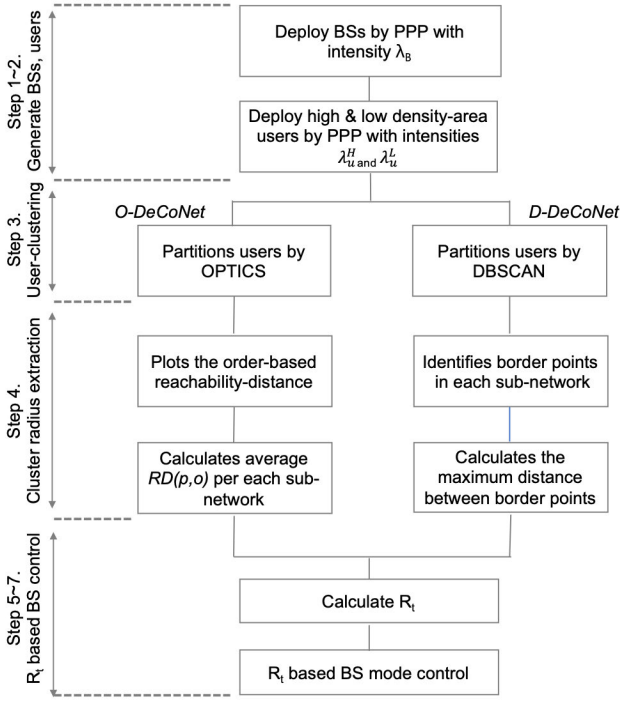

FIGURE 3. Block diagram of the proposed DeCoNet algorithm.

in the D-DeCoNet algorithm. After calculating r_t based on r_c according to Step 5, the BSs satisfying the condition of $\text{Dist}(o, i) < r_t$ are changed into the sleep mode.

IV. SIMULATION RESULTS AND DISCUSSION

A. SIMULATION ENVIRONMENTS

The total network size is 1 km^2 and the number of high user-density areas is assumed as 3. The capacity of each BS is 100. Thus, each BS is able to support a maximum of 100 users. Depending on the type of the proposed DeCoNet algorithm (O-DeCoNet, D-DeCoNet), the sizes of the subnetworks could be different. For performance comparison, we consider two conventional algorithms, namely, the ACEnet algorithm [7] and the always-awake (AA) algorithm. In ACEnet, the BS mode control is performed according to the user density of the entire network. This algorithm does not consider the difference in user density for each unit area. Furthermore, in the AA algorithm, the status of every BS must always be awake regardless of the user density and status.

We consider fixed and random locations of the high user-density areas in the simulations. The user density of the high-density area and low-density area are $\lambda_u^H = 4 \sim 30 \times 10^3$ and $\lambda_u^L = 1 \times 10^3$, respectively. If we assume the radius of a high-density area as 100 m, the connection density of this area becomes approximately 0.95 user/m^2. This value is almost the same as the target value of the connection density in IMT-2020, 1 user/m^2 [1]. The BS density (λ_B) is 0.1×10^3, and the transmission power of the BS is 0.25 W. The details of the simulation parameters are shown in Table. 1.

TABLE 1. Simulation parameters.

Parameter	Value
Network Size	1 km × 1 km
Total Bandwidth (B)	10 MHz
Number of High-Density Areas	3
Deployment Strategy for High-Density Areas	Fixed & Random
User Density of High-Density Area (λ_u^H)	$4 \sim 30 \times 10^3$
User Density of Low-Density Area (λ_u^L)	1×10^3
BS Density (λ_B)	0.1×10^3
Path-loss Exponent (ν)	3.5
BS Transmission Power (P_{tx})	0.25 W
Power Consumption by Circuit (P_{c})	5.4 W
Power Consumption in Standby State (P_{o})	0.7 W
Amplification Efficiency (σ)	0.23
BS capacity (μ_B)	100

B. PERFORMANCE METRICS

To evaluate the performance of the proposed (O-DeCoNet and D-DeCoNet) and conventional (ACEnet and AA) algorithms under various network conditions, we consider four performance metrics, namely, energy per information bit (η_I), power per area unit (η_A), area throughput (T_A), and energy efficiency (η_E). Here, η_I and η_A are utilized to evaluate the energy efficiency at the network level of the UDN environment where the BSs and the users are densely distributed [30], [31].

The unit of η_I is W/bps, and this metric is known to be suitable for the performance evaluation of urban environments. The unit of η_A is W/km^2, and this metric is widely utilized for the performance evaluation of suburban and rural environments. Moreover, η_I and η_A are represented as

$$\eta_I = \frac{\sum_{i\in\mathbb{S}_B^{\text{awake}}} P_B(i)}{\sum_{i\in\mathbb{S}_B^{\text{awake}}}\sum_{j\in\mathbb{S}_{u,j}} B\log(1+\gamma_j^i)}\ [\text{W/bps}],$$
$$\eta_A = \frac{\sum_{i\in\mathbb{S}_B^{\text{awake}}} P_B(i)}{\sum_{i\in\mathbb{S}_B^{\text{awake}}} \chi_B(i)}\ [\text{W/km}^2]. \tag{11}$$

Here, γ_j^i is the signal-to-interference-plus-noise ratio (SINR) of user j against BS i, and P_B can be obtained by calculating the total amount of power consumed by the BS as follows: $(P_B = (1/\sigma) \cdot P_{\text{tx}} + P_c + P_o)$. In this equation, σ is the amplification efficiency and P_{tx} is the transmission power of the BS. P_c and P_o denote the power consumed by the circuit and the power consumed in the standby state, respectively. Furthermore, χ_B is the size of each BS area formed by Voronoi tessellation.

In addition, T_A and η_E can be calculated as

$$T_A = \frac{\sum_{i\in\mathbb{S}_B^{\text{awake}}}\sum_{j\in\mathbb{S}_{u,j}} B\log(1+\gamma_j^i)}{\sum_{i\in\mathbb{S}_B^{\text{awake}}} \chi_B(i)}\ [\text{bps/km}^2],$$
$$\eta_E = \frac{\sum_{i\in\mathbb{S}_B^{\text{awake}}}\sum_{j\in\mathbb{S}_{u,j}} B\log(1+\gamma_j^i)}{\sum_{i\in\mathbb{S}_B^{\text{awake}}} P_B(i)}\ [\text{bit/J}]. \tag{12}$$

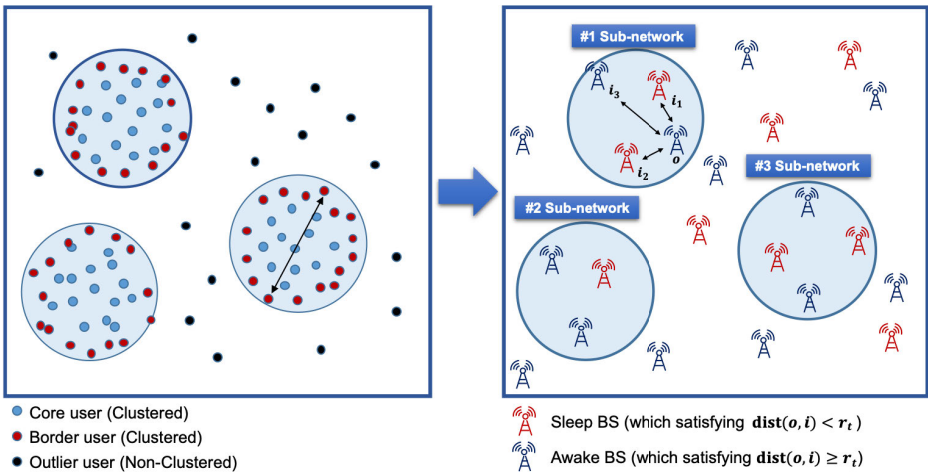

FIGURE 4. Density-based user clustering for creating subnetworks (left); Thinning-based BS status adjustment (right).

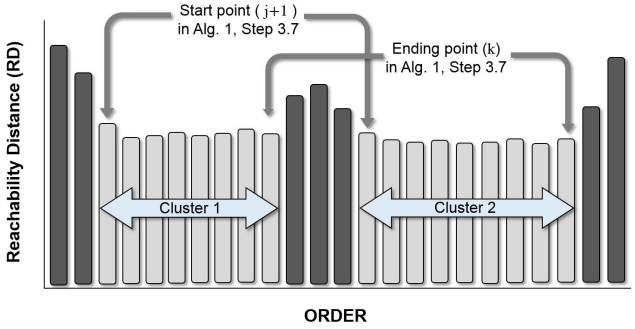

FIGURE 5. Example of RD plot in O-DeCoNet.

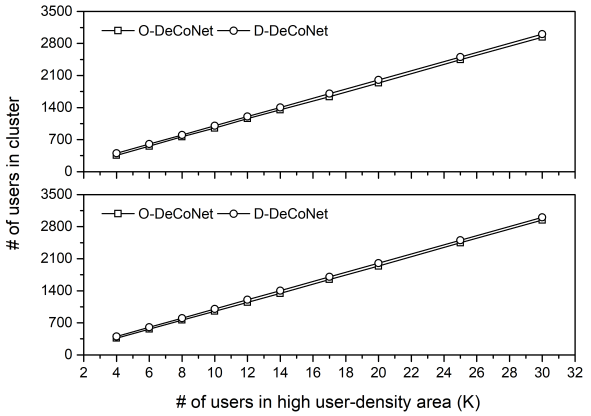

FIGURE 6. Average number of users in each cluster; random deployment (up) and fixed deployment (down).

C. SIMULATION RESULTS

Fig. 6 shows the results of the number of users included in each cluster after applying the clustering algorithms, OPTICS and DBSCAN. The results of D-DeCoNet are well matched with the user density of the high user-density area. On the other hand, O-DeCoNet obtains a relatively lower value than that of D-DeCoNet because the cluster points are excluded in the reachability-distance plot corresponding to the parameter of OPTICS (ξ). Here, ξ is a steepness parameter to extract clusters as described in Step 3.7 in Algorithm 1. In a reachability-distance plot, the user $i+1$ satisfying $RD_i \times (1-\xi) \geq RD_{i+1}$ becomes the start point of a cluster, and the user j satisfying $RD_j \leq RD_{j+1} \times (1-\xi)$ becomes the end point of the cluster. All successive points between the start point $i+1$ and the end point j form a cluster. The number of users belonging to each cluster could vary by the steepness parameter ξ. That is, O-DeCoNet would create relatively small clusters compared to D-DeCoNet. This reduces the utilization of BSs in the high user-density areas. Accordingly, D-DeCoNet has the highest throughput among these algorithms.

Fig. 7 shows the simulation results with respect to the area throughput, energy efficiency, energy per information bit, and power per area unit of O-DeCoNet, D-DeCoNet, ACEnet, and AA in the case of fixed deployment of high user-density areas. Fig. 7(a) shows the area throughput according to the average number of users in high user-density areas. The proposed O-DeCoNet and D-DeCoNet algorithms perform thinning operations to put the neighboring BSs into sleep mode depending on the user density. Consequently, the total amount of interference generated by the neighboring BSs can be reduced because of these mode changes. These findings indicate the throughput improvement of the proposed O-DeCoNet and D-DeCoNet algorithms. In O-DeCoNet and D-DeCoNet, the BS mode control algorithm is adaptively utilized according to the active user density because the subnetworks are constructed using density-based clustering algorithms such as OPTICS and DBSCAN. Therefore, the proposed algorithms outperform the conventional AA and ACEnet algorithms with respect to the area throughput. Moreover, ACEnet has the smallest T_A because this algorithm does not consider the difference in the user density in the entire network. Furthermore, the AA algorithm causes a severe interference problem because all the BSs in the entire

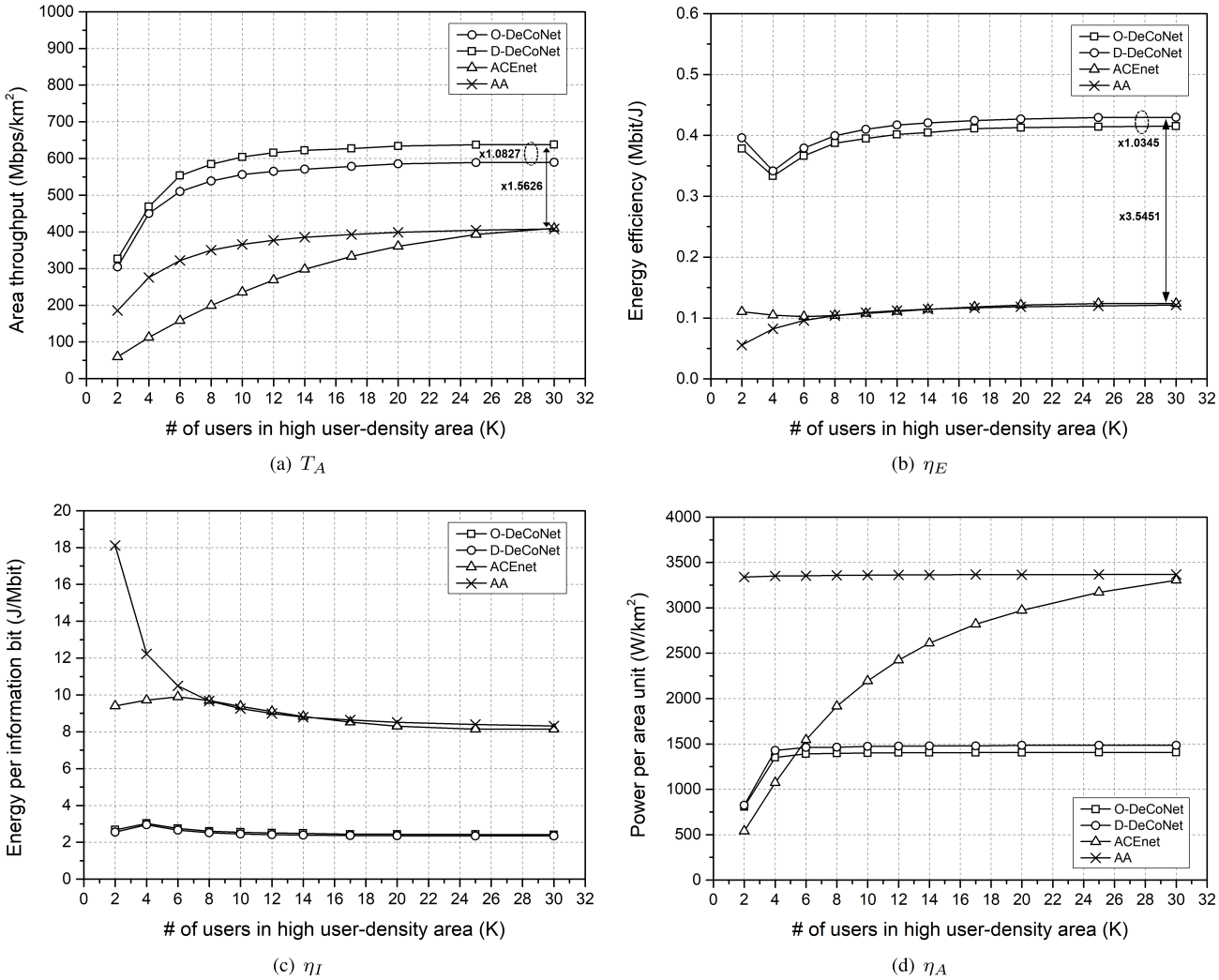

FIGURE 7. Area throughput, energy efficiency, energy per information bit, and power per area unit of O-DeCoNet, D-DeCoNet, ACEnet, and AA in the case of fixed placement of high user-density areas.

network are always kept in the awake state. The reason for the slight performance difference between O-DeCoNet and D-DeCoNet is the difference in the shape of the clusters formed by each clustering algorithm.

Fig. 7(b) shows the energy efficiency according to the average number of users in high user-density areas. Because ACEnet does not consider the user distribution, this algorithm has an energy wastage problem in low-density areas. It causes performance degradation in terms of energy efficiency. Due to similar reasons, the AA algorithm has the lowest energy efficiency among these algorithms. On the other hand, because the proposed O-DeCoNet and D-DeCoNet algorithms control the BSs adaptively considering the user density by area, these algorithms achieve better performance than the conventional ACEnet and AA algorithms. The difference in cluster shape in the high user-density areas causes a slight difference in η_E, as shown in Fig. 7(b). Fig. 7(d) shows the power per area unit according to the average number of users in high user-density areas. From this figure, we can find the total power consumed by the BSs. In the AA algorithm, all the BSs are always kept in the awake mode because there is no thinning algorithm. In this algorithm, the total amount of power consumed in the BSs does not change regardless of the change in the user density. In addition, O-DeCoNet and D-DeCoNet have lower energy efficiency when the number of users in a high user-density area is $4K$ compared to the case of $2K$. This occurs because the relative increment ratio of the throughput in the case of $2K$ is larger than the decrement ratio of the amount of saved power due to the BS mode changes compared to the case of $4K$.

On the other hand, O-DeCoNet, D-DeCoNet, and ACEnet utilize the thinning operation to adjust the status of BSs in consideration of the user density. However, because the ACEnet algorithm does not partition the areas according to the user density, η_A increases continuously until it reaches the η_A of the AA algorithm. That is, the total number of users

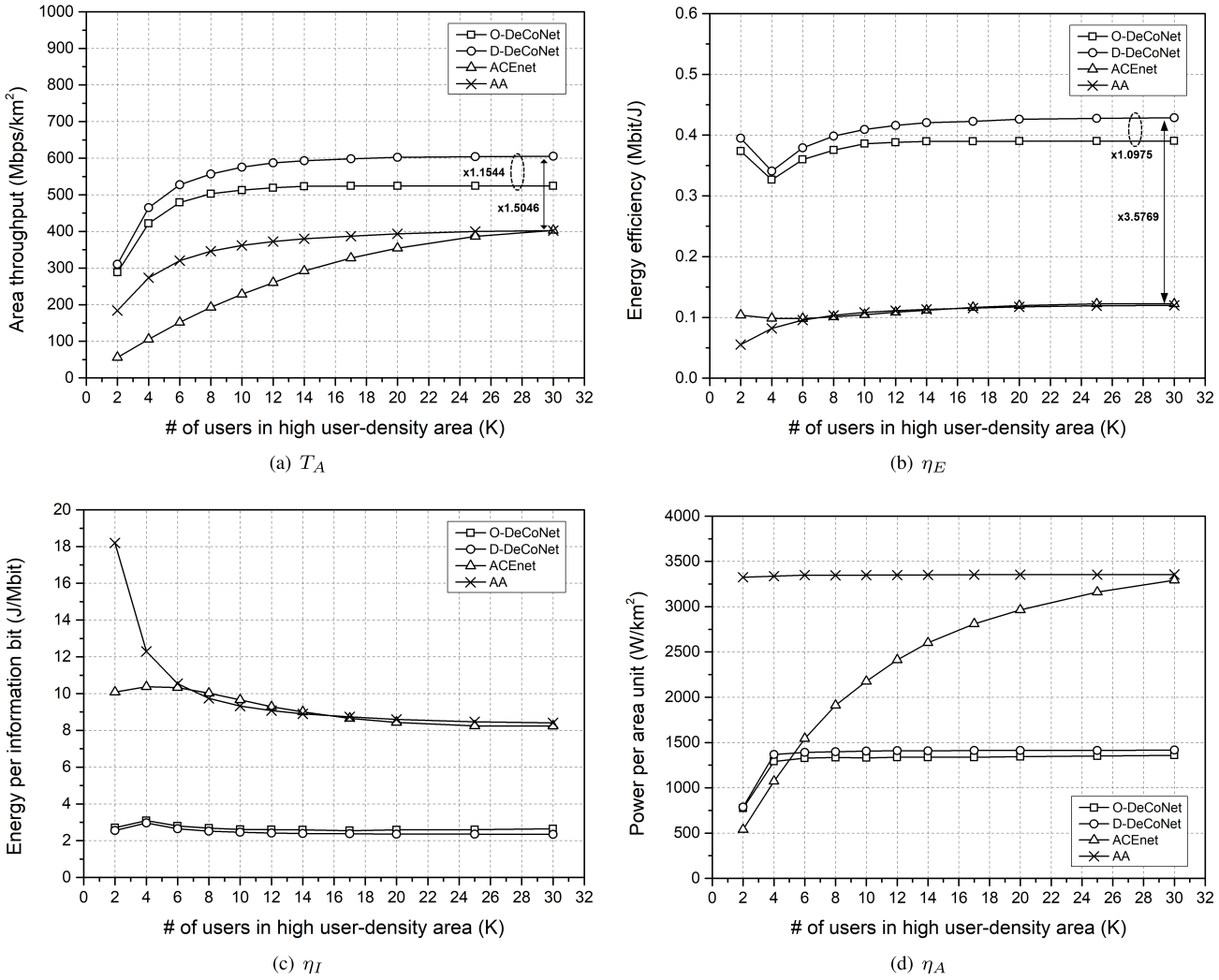

(a) T_A (b) η_E (c) η_I (d) η_A

FIGURE 8. Area throughput, energy efficiency, energy per information bit, and power per area unit of O-DeCoNet, D-DeCoNet, ACEnet, and AA in the case of random placement of high user-density areas.

is 90.5K, and the number of users in each high user-density area is 30K; the η_A of ACEnet is almost the same as the η_A of AA. In addition, when the number of users in the high user-density area becomes 4K, all the BSs in this area should become awake. Accordingly, from this point, η_A saturations occur in the O-DeCoNet and D-DeCoNet algorithms. We can observe a similar performance tendency in Fig.7(c). Figs. 7(c) and 7(d) show that the proposed DeCoNet algorithms have significant advantages in terms of power consumption.

Fig. 8 shows the simulation results with respect to the area throughput, energy efficiency, energy per information bit, and power per area unit of O-DeCoNet, D-DeCoNet, ACEnet, and AA when the high user-density areas are randomly deployed. The AA and ACEnet algorithms exhibit similar performance regardless of the placement of the high user-density areas. As shown in Fig. 8(a), the area throughput of the proposed DeCoNet algorithms in the case of random deployment of high user-density areas is smaller than that of the proposed DeCoNet algorithms in the case of fixed deployment of high user-density areas. This is the reason why the inter-distance between high user-density areas in the case of random deployment could be less than that in the case of fixed deployment. That is, relatively more severe interference can be generated from adjacent BSs in the case of random deployment.

From the reachability-distance plot of the proposed O-DeCoNet algorithm, it can be seen that when the inter-distance between the start point and end point of the cluster decreases, the size of the cluster also decreases. Accordingly, the number of BSs that need to be awake in this cluster could decrease. Consequently, the area throughput in Fig. 8(a) is relatively small compared to that in Fig. 7(a). That is, as the awake BSs become closer, the interference generated by the users included in these awake BSs could increase. Therefore, the gap of η_A between O-DeCoNet and D-DeCoNet in Fig. 8(d) is decreased compared to that in Fig. 7(d). On the other hand, the gap of η_E between

O-DeCoNet and D-DeCoNet increases from $\times 1.0345$ to $\times 1.0975$.

V. CONCLUSIONS

To improve the energy efficiency in ultra-dense cellular IoT networks, we proposed two novel DeCoNet algorithms: OPTICS-based DeCoNet and DBSCAN-based DeCoNet. To consider the difference in the user density per area, we partitioned the entire network into several subnetworks. After partitioning, we exploited thinning operations to determine the status of the BSs. The thinning radii that were required to adjust the status of the BSs were calculated from the distance between the outermost nodes in the case of D-DeCoNet and the reachability-distance in the case of O-DeCoNet. Through extensive computer simulations, we showed that the proposed O-DeCoNet and D-DeCoNet algorithms outperform the conventional ACEnet and AA algorithms in terms of average area throughput, energy efficiency, energy per information bit, and power consumption per unit area in the case of fixed and random placements of high user-density areas.

REFERENCES

[1] *IMT Vision—Framework and Overall Objectives of the Future Development of IMT for 2020 and Beyond*, document Recommendation ITU-R M.2083-0, Sep. 2015, pp. 1–19.
[2] A. Zanella, N. Bui, A. Castellani, L. Vangelista, and M. Zorzi, "Internet of Things for smart cities," *IEEE Internet Things J.*, vol. 1, no. 1, pp. 22–32, Feb. 2014.
[3] K. Lee, J.-P. Hong, H.-H. Choi, and M. Levorato, "Adaptive wireless-powered relaying schemes with cooperative jamming for two-hop secure communication," *IEEE Internet Things J.*, vol. 5, no. 4, pp. 2793–2803, Aug. 2018.
[4] C. Pan, M. Elkashlan, J. Wang, J. Yuan, and L. Hanzo, "User-centric C-RAN architecture for ultra-dense 5G networks: Challenges and methodologies," *IEEE Commun. Mag.*, vol. 56, no. 6, pp. 14–20, Jun. 2018.
[5] L. Wang, K.-K. Wong, S. Jin, G. Zheng, and R. W. Heath, "A new look at physical layer security, caching, and wireless energy harvesting for heterogeneous ultra-dense networks," *IEEE Commun. Mag.*, vol. 56, no. 6, pp. 49–55, Jun. 2018.
[6] T. Zhang, J. Zhao, L. An, and D. Liu, "Energy efficiency of base station deployment in ultra dense HetNets: A stochastic geometry analysis," *IEEE Wireless Commun. Lett.*, vol. 5, no. 2, pp. 184–187, Apr. 2016.
[7] W. Lee, B. C. Jung, and H. Lee, "ACEnet: Approximate thinning-based judicious network control for energy-efficient ultra-dense networks," *Energies*, vol. 11, no. 5, p. 1307, May 2018.
[8] Q. Li, G. Wu, and R. Q. Hu, "Analytical study on network spectrum efficiency of ultra dense networks," in *Proc. IEEE 24th Annu. Int. Symp. Pers., Indoor, Mobile Radio Commun. (PIMRC)*, Sep. 2013, pp. 2764–2768.
[9] Q. Ren, J. Fan, X. Luo, Z. Xu, and Y. Chen, "Analysis of spectral and energy efficiency in ultra-dense network," in *Proc. IEEE Int. Conf. Commun. Workshop (ICCW)*, Jun. 2015, pp. 2812–2817.
[10] S. Tombaz, M. Usman, and J. Zander, "Energy efficiency improvements through heterogeneous networks in diverse traffic distribution scenarios," in *Proc. 6th Int. ICST Conf. Commun. Netw. China (CHINACOM)*, Aug. 2011, pp. 708–713.
[11] F. Richter, A. J. Fehske, and G. P. Fettweis, "Energy efficiency aspects of base station deployment strategies for cellular networks," in *Proc. IEEE 70th Veh. Technol. Conf. Fall*, Sep. 2009, pp. 1–5.
[12] Z. Hasan, H. Boostanimehr, and V. K. Bhargava, "Green cellular networks: A survey, some research issues and challenges," *IEEE Commun. Surveys Tuts.*, vol. 13, no. 4, pp. 524–540, Apr. 2011.
[13] D. Lopez-Perez, M. Ding, H. Claussen, and A. H. Jafari, "Towards 1 Gbps/UE in cellular systems: Understanding ultra-dense small cell deployments," *IEEE Commun. Surveys Tuts.*, vol. 17, no. 4, pp. 2078–2101, Jun. 2015.
[14] G. P. Koudouridis, H. Gao, and P. Legg, "A centralised approach to power on-off optimisation for heterogeneous networks," in *Proc. IEEE Veh. Technol. Conf. (VTC Fall)*, Sep. 2012, pp. 1–5.
[15] L. Saker, S. E. Elayoubi, R. Combes, and T. Chahed, "Optimal control of wake up mechanisms of femtocells in heterogeneous networks," *IEEE J. Sel. Areas Commun.*, vol. 30, no. 3, pp. 664–672, Apr. 2012.
[16] H. Zhang, S. Huang, C. Jiang, K. Long, V. C. M. Leung, and H. V. Poor, "Energy efficient user association and power allocation in millimeter-wave-based ultra dense networks with energy harvesting base stations," *IEEE J. Sel. Areas Commun.*, vol. 35, no. 9, pp. 1936–1947, Sep. 2017.
[17] Z. Jian, W. Muqing, and Z. Min, "Energy-efficient switching on/off strategies analysis for dense cellular networks with partial conventional base-stations," *IEEE Access*, vol. 8, pp. 9133–9145, 2020.
[18] H. Celebi, Y. Yapici, I. Guvenc, and H. Schulzrinne, "Load-based on/off scheduling for energy-efficient delay-tolerant 5G networks," *IEEE Trans. Green Commun. Netw.*, vol. 3, no. 4, pp. 955–970, Dec. 2019.
[19] L. Liang, W. Wang, Y. Jia, and S. Fu, "A cluster-based energy-efficient resource management scheme for ultra-dense networks," *IEEE Access*, vol. 4, pp. 6823–6832, 2016.
[20] Y. Lin, R. Zhang, L. Yang, and L. Hanzo, "Modularity-based user-centric clustering and resource allocation for ultra dense networks," *IEEE Trans. Veh. Technol.*, vol. 67, no. 12, pp. 12457–12461, Dec. 2018.
[21] J. G. Andrews, F. Baccelli, and R. K. Ganti, "A tractable approach to coverage and rate in cellular networks," *IEEE Trans. Commun.*, vol. 59, no. 11, pp. 3122–3134, Nov. 2011.
[22] S. G. Foss and S. A. Zuyev, "On a Voronoi aggregative process related to a bivariate Poisson process," *Adv. Appl. Probab.*, vol. 28, no. 4, pp. 965–981, Dec. 1996.
[23] H. Jia, J. Chen, X. Ge, and Q. Li, "Switch-off strategy of base stations in HCPP random cellular networks," in *Proc. IEEE Int. Conf. Commun. (ICC)*, May 2016, pp. 1–6.
[24] G. Alfano, M. Garetto, and E. Leonardi, "New insights into the stochastic geometry analysis of dense CSMA networks," in *Proc. IEEE INFOCOM*, Apr. 2011, pp. 2642–2650.
[25] B. Matern, *Spatial Variation*, 2nd ed. New York, NY, USA: Springer-Verlag, 1986.
[26] M. Haenggi, "Mean interference in hard-core wireless networks," *IEEE Commun. Lett.*, vol. 15, no. 8, pp. 792–794, Aug. 2011.
[27] H. S. Dhillon, R. K. Ganti, F. Baccelli, and J. G. Andrews, "Modeling and analysis of K-tier downlink heterogeneous cellular networks," *IEEE J. Sel. Areas Commun.*, vol. 30, no. 3, pp. 550–560, Apr. 2012.
[28] M. Ester, H.-P. Kriegel, J. Sander, and X. Xu, "A density-based algorithm for discovering clusters in large spatial databases with noise," in *Proc. 2nd Int. Conf. Knowl. Discovery Data Mining*, Portland, OR, USA, Aug. 1996, pp. 226–231.
[29] M. Ankerst, M. Breunig, H.-P. Kriegel, and J. Sander, "OPTICS: Ordering points to identify the clustering structure," in *Proc. ACM SIGMOD Int. Conf. Manage. Data*, Philadelphia, PA, USA, Jun. 1999, pp. 49–60.
[30] P. Popovski, V. Braun, and Z. Ren, "Deliverable D1.1: Scenarios, requirements and KPIs for 5G mobile and wireless system," FP7 METIS, Tech. Rep. METIS ICT-317669-METIS/D1.1, Apr. 2013, pp. 1–75.
[31] M. A. Imran, J. Alonso-Rubio, G. Auer, M. Boldi, M. Braglia, P. Fazekas, D. Ferling, A. Fehske, P. Frenger, R. Gupta, and E. Katranaras, "Deliverable D2.4: Most suitable efficiency metrics and utility functions," FP7 EARTH, Tech. Rep. FP7 EARTH Project INFSO-ICT-247733 EARTH, Jan. 2012, pp. 1–55.

WONSEOK LEE received the B.S. and M.S. degrees in electronic engineering from Hankyong National University (HKNU), Anseong, South Korea, in 2016 and 2018, respectively. Since 2019, he has been with the Innovative Technology Lab (ITL) Inc., Seoul, South Korea. His research interests include 5G mobile communications, the Internet of Things, and stochastic geometry. He was a recipient of the Best Paper Award at the Korean Institute of Communications and Information Sciences (KICS) Summer Conference, in 2017.

BANG CHUL JUNG (Senior Member, IEEE) received the B.S. degree in electronics engineering from Ajou University, Suwon, South Korea, in 2002, and the M.S. and Ph.D. degrees in electrical and computer engineering from the Korea Advanced Institute of Science and Technology (KAIST), Daejeon, South Korea, in 2004 and 2008, respectively. He was a Senior Researcher/Research Professor with the KAIST Institute for Information Technology Convergence, Daejeon, from 2009 to 2010. From 2010 to 2015, he was a Faculty Member with Gyeongsang National University. He is currently an Associate Professor with the Department of Electronics Engineering, Chungnam National University, Daejeon. His research interests include 5G mobile communication systems, statistical signal processing, opportunistic communications, compressed sensing, interference management, interference alignment, random access, relaying techniques, device-to-device networks, in-network computation, and network coding. He was a recipient of the Fifth IEEE Communication Society Asia–Pacific Outstanding Young Researcher Award, in 2011. He was also a recipient of the Bronze Prize at the Intel Student Paper Contest, in 2005, the First Prize at the KAIST's Invention Idea Contest, in 2008, the Bronze Prize at the Samsung Humantech Paper Contest, in 2009, and the Outstanding Paper Award at the Spring Conference of Korea Institute of Information and Communication Engineering, in 2015. He received the Haedong Young Scholar Award, in 2015, which is sponsored by the Haedong Foundation and given by the Korea Institute of Communications and Information Science.

HOWON LEE (Member, IEEE) received the B.S., M.S., and Ph.D. degrees in electrical and computer engineering from the Korea Advanced Institute of Science and Technology (KAIST), Daejeon, South Korea, in 2003, 2005, and 2009, respectively. From 2009 to 2012, he was a Senior Research Staff/Team Leader of the Knowledge Convergence Team, KAIST Institute for Information Technology Convergence (KI-ITC). Since 2012, he has been with the Department of Electrical, Electronic and Control Engineering (EECE) and the Institute for IT Convergence (IITC), Hankyong National University (HKNU), Anseong, South Korea. His current research interests include 5G wireless communications, ultra-dense distributed networks, in-network computations for 3D images, cross-layer radio resource management, machine learning, and the Internet of Things. He was a recipient of the Joint Conference on Communications and Information (JCCI) 2006 Best Paper Award and the Bronze Prize at the Intel Student Paper Contest, in 2006. He was also a recipient of the Telecommunications Technology Association (TTA) Paper Contest Encouragement Award, in 2011, the Best Paper Award at the Korean Institute of Communications and Information Sciences (KICS) Summer Conference, in 2015, the Best Paper Award at the KICS Fall Conference, in 2015, the Honorable Achievement Award from 5G Forum Korea, in 2016, the Best Paper Award at the KICS Summer Conference, in 2017, the Best Paper Award at the KICS Winter Conference, in 2018, the Best Paper Award at the KICS Summer Conference, in 2018, and the Best Paper Award at the KICS Winter Conference, in 2020. He received the Minister's Commendation by the Minister of Science and ICT, in 2017.